ACS APPLIED MATERIALS & INTERFACES

Research Article

www.acsami.org

Tetrahedral DNA Nanostructure-Based MicroRNA Biosensor Coupled with Catalytic Recycling of the Analyte

Peng Miao,*[,†,‡] Bidou Wang,[†] Xifeng Chen,[†] Xiaoxi Li,[§] and Yuguo Tang*[,†,‡]

[†]CAS Key Lab of Bio-Medical Diagnostics, Suzhou Institute of Biomedical Engineering and Technology, Chinese Academy of Sciences, Suzhou 215163, China

[‡]University of Chinese Academy of Sciences, Beijing 100049, China

[§]Department of Biochemistry and National Key Laboratory of Pharmaceutical Biotechnology, Nanjing University, Nanjing 210093, China

Supporting Information

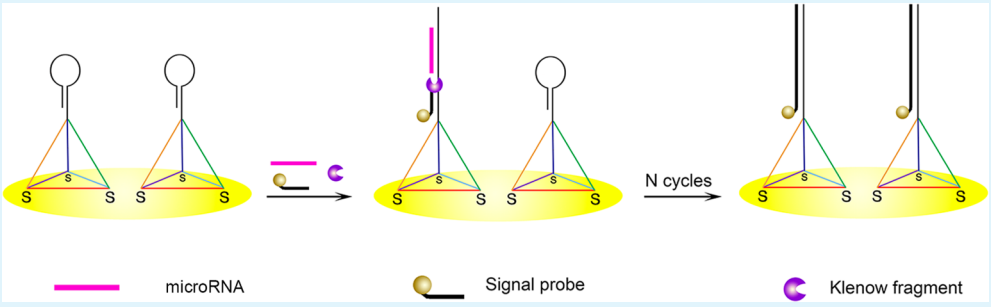

ABSTRACT: MicroRNAs are not only important regulators of a wide range of cellular processes but are also identified as promising disease biomarkers. Due to the low contents in serum, microRNAs are always difficult to detect accurately . In this study, an electrochemical biosensor for ultrasensitive detection of microRNA based on tetrahedral DNA nanostructure is developed. Four DNA single strands are engineered to form a tetrahedral nanostructure with a pendant stem-loop and modified on a gold electrode surface, which largely enhances the molecular recognition efficiency. Moreover, taking advantage of strand displacement polymerization, catalytic recycling of microRNA, and silver nanoparticle-based solid-state Ag/AgCl reaction, the proposed biosensor exhibits high sensitivity with the limit of detection down to 0.4 fM. This biosensor shows great clinical value and may have practical utility in early diagnosis and prognosis of certain diseases.

KEYWORDS: *microRNA, tetrahedral DNA nanostructure, strand displacement reaction, silver nanoparticles, linear sweep voltammetry*

INTRODUCTION

MicroRNAs belong to small endogenous noncoding RNAs and regulate almost every cellular process, including cell growth, differentiation, apoptosis, and autophagy at the post-transcriptional level.[1−3] Recently, the investigation of biological roles of microRNA and potential clinical applications have been paid more and more attention.[4−7] It is reported that the variation of numerous abnormal cellular processes accompanies the up- or down-regulation of microRNA expression.[8] Therefore, microRNAs may provide a rich platform of biomarkers associating different diseases and may greatly improve disease diagnosis in decreasing the percentage of false positives or replacing uncomfortable traditional diagnostic procedures.[9,10] For example, although colonoscopy is the gold standard for the detection of colorectal cancer, the resulting discomfort makes it unsuitable for cancer screening in the general population. Plasma miR-409-3p, miR-7, and miR-93 levels can be detected and used to distinguish colorectal cancer from healthy groups with high diagnostic accuracy.[11] Lung cancer is a major cause of death not only in China but also in many western countries. Most screening methods involve invasive operations and are inaccurate. The level of miRNA-21 is found to be much higher in the serum or exhaled breath condensate of non-small cell lung cancer patients and may have significant diagnostic value.[12]

At present, tremendous progress has been made for the detection of microRNA.[13−15] Northern blotting is widely accepted as the gold standard. Quantitative polymerase chain reaction (qPCR) is also a popular technique for microRNA detection.[16] However, these methods are labor intensive or require expensive instruments and reagents, which cannot meet the high standards for point-of-care testing (POCT) of microRNAs. Electrochemical biosensors have been utilized in many bioanalytical applications, owing to the advantages of simplicity, low cost, high sensitivity, and fast response compared with other techniques, such as fluorescent

Received: January 17, 2015
Accepted: March 4, 2015
Published: March 4, 2015

DOI: 10.1021/acsami.5b01508
ACS Appl. Mater. Interfaces 2015, 7, 6238−6243

assays.[17−23] Therefore, electrochemical techniques are promising analytical tools. However, due to the features of low contents, short sequences, and high sequence homology among family members of microRNAs, signal amplification strategies should be included in electrochemical detection of microRNA.[24,25] Moreover, optimization of electrode surface modification can also help improve the sensitivity and specificity.[26,27]

Herein, we fabricate an electrochemical biosensor for ultrasensitive detection of microRNA based on tetrahedral DNA nanostructure coupled with catalytic recycling of microRNA. The application of tetrahedral DNA nanostructure makes DNA monolayers well aligned on the surface of electrode with controlled density and orientation,[28,29] which cuts the "backfilling" process (i.e., mercaptohexanol incubation) and simplifies the immobilization steps.[30] The reactivity and accessibility can also be improved due to the DNA scaffold.[31] In addition, strand displacement polymerization is employed which leads to the recycling of microRNA and the enzymatic amplification contributes to the high sensitivity of this method.[32,33] The limit of detection (LOD) is as low as 0.4 fM. Single-base mismatch can be distinguished. This method also performs well for the detection of microRNA levels of breast cancer patients. Therefore, it offers a great promise for early diagnosis and prognosis of certain diseases.

EXPERIMENTAL SECTION

Materials and Chemicals. Tris(2-carboxyethyl)phosphine hydrochloride (TCEP), diethypyrocarbonate (DEPC), silver nitrate ($AgNO_3$), sodium borohydride ($NaBH_4$), and trisodium citrate were purchased from Sigma-Aldrich (St. Louis, MO). Klenow fragment was obtained from New England Biolabs, Ltd. (Beijing, China). Human serum samples were supplied by a local hospital (Suzhou, China). Other reagents were of analytical grade and were used as received. All solutions were prepared with Milli-Q water (18 MΩ·cm resistivity) from a Millipore system. Oligonucleotides used were synthesized and purified by Takara Biotechnology Co., Ltd. (Dalian, China). The corresponding sequences are listed in Table 1.

Preparation of AgNPs-Labeled Signal Probe. Bare AgNPs were prepared by the borohydride reduction of $AgNO_3$ following the previously reported protocol.[34] Briefly, 100 mL of $AgNO_3$ and trisodium citrate solution was prepared with the concentration of 0.25 mM. Then, it was mixed with 3 mL of $NaBH_4$ solution (10 mM) under stirring for 30 min. The mixed solution exhibited the color of bright yellow and were left overnight in the dark. The prepared AgNPs were then purified by three cycles of centrifugation at 12000*g* for 30 min. Afterward, AgNPs were incubated in signal probe (10 μM) for 24 h and were then further purified by centrifugation.

Self-Assembly of Tetrahedral DNA Nanostructure at Gold Electrode. The gold electrode with the diameter of 2 mm was cleaned prior to any modification.[35] It was first soaked in piranha solution (98% H_2SO_4, 30% H_2O_2 = 3:1) for 5 min.

***Caution**: Piranha solution reacts violently with organic solvents and should be handled with great care.*

Then, it was polished on P5000 sand paper and alumina slurry (1, 0.3, and 0.05 μm). Afterward, the electrode was cleaned by ultrasonicating in ethanol and double-distilled water. The electrode was then treated with 50% HNO_3 for 30 min and electrochemically cleaned with 0.5 M H_2SO_4.

The tetrahedral DNA nanostructure consisted of four DNA strands were formed based on a modified protocol.[36] Tetrahedron A, B, C, and D were separately dissolved in the buffer solution (10 mM Tris-HCl, 10 mM TCEP, 50 mM $MgCl_2$, pH 8.0) with the concentration of 4 μM. To form the tetrahedral DNA nanostructure, wee mixed 25 μL of each strands, heated them to 95 °C for 2 min, and then cooled them to 4 °C. Afterward, 10 μL of the tetrahedral DNA nanostructure was dipped on the cleaned gold electrode and the reaction lasted for 8 h.

Table 1. DNA and RNA Sequences Used in This Work

Name	Sequence (5′-3′)
tetrahedron A	ATGTGTTAGTATCAACATCAGTCTGATAAGCTATACTAACACATTTTACATTCCTAAGTCTGAAACATTACAGCTTGCTACACGAGAAGAGCCGCCATAGTA
tetrahedron B	SH-C_6-TATCACCAGGCAGTTGACAGTGTAGCAAGCTGTAATAGATGCGAGGGTCCAATAC
tetrahedron C	SH-C_6-TCAACTGCCTGGTGATAAAACGACACTACGTGGGAATCTACTATGGCGGCTCTTC
tetrahedron D	SH-C_6-TTCAGACTTAGGAATGTGCTTCCCACGTAGTGTCGTTTGTATTGGACCCTCGCAT
miRNA-21	UAGCUUAUCAGACUGAUGUUGA
mismatch 1	UCGCUUAUCAGACUGAUGUUGA
mismatch 2	UAGCUUAUCAGTCUGAUGUUGA
mismatch 3	UAGCUUAUCAGACUGAUGUAGA
signal probe	AgNPs-NH_2−C_6-GTGTTAGT

DOI: 10.1021/acsami.5b01508
ACS Appl. Mater. Interfaces 2015, 7, 6238−6243

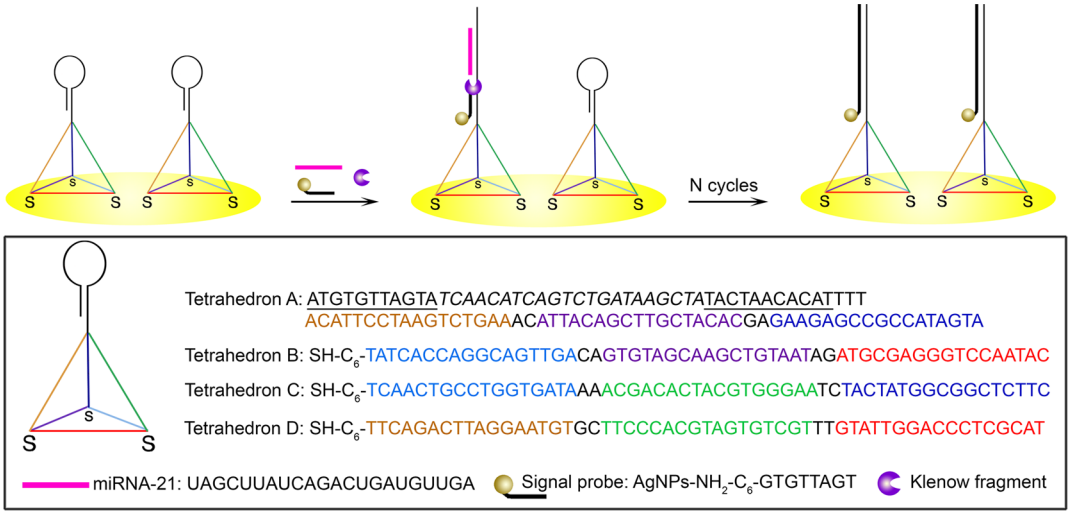

Figure 1. Schematic illustration of the tetrahedral DNA nanostructure-based microRNA biosensor.

Strand Displacement and MicroRNA Recycling. We prepared 50 μL polymerase reaction solution (10 mM Tris-HCl, 50 mM NaCl, 10 mM $MgCl_2$, 1 mM dithiothreitol) containing 5 units of Klenow fragment, 2.5 nmol of dNTPs, 1 nmol of signal probe and different amount of microRNA. The tetrahedral DNA nanostructure modified electrode was incubated in the above polymerase reaction solution at 37 °C for 4 h.

Electrochemical Measurements. All electrochemical experiments were carried out on a CHI 660D electrochemical workstation (CH Instruments, Shanghai, China). A three-electrode system was used, which contained the platinum auxiliary electrode, the Ag/AgCl reference electrode, and the tetrahedral DNA nanostructure modified working electrode. Electrochemical impedance spectra (EIS) were performed in 5 mM $Fe(CN)_6^{3-/4-}$ with 1 M KNO_3. The bias potential was 0.204 V, the amplitude was 5 mV, and the frequency range was from 1 to 100 000 Hz. Linear sweep voltammetry (LSV) experiments were performed at room temperature. The scan rate was 100 mV/s, and the electrolyte was 0.1 M KCl.

RESULTS AND DISCUSSION

Sensing Principle. Generally, a tetrahedral DNA nanostructure is designed with a pendant stem-loop to recognize target microRNA. As shown in Figure 1, four DNA single strands, tetrahedron A, B, C, and D, are engineered to form the six edges of the tetrahedral nanostructure through hybridization. Three vertices of tetrahedron are modified with thiols, which facilitates the immobilization on the gold electrode surface.[37] Tetrahedron A also includes the stem−loop sequence, in which the underlined parts hybridize with each other, and the italic part is the complementary sequence of target microRNA. Because tetrahedral DNA nanostructure-bottomed scaffold supports the stem-loop in the upright orientation, molecular recognition efficiency can be largely enhanced. In the presence of microRNA, the loop of tetrahedron A is opened by hybridization, which also releases single-stranded stem part that is complementary to the sequence within the signal probe. The signal probe is labeled with AgNPs, the diameter of which is around 4 nm (Figure S1, Supporting Information). Because the $-(CH_2)_6-$ spacer between AgNPs and DNA sequence in the signal probe is flexible, the hybridization between signal probe and tetrahedron A is feasible. Moreover, Klenow fragment can then initiate the polymerization of signal probe and the lengthening of new strand releases microRNA, which opens more loops, helps more signal probe hybridizations, and triggers new strand displacement polymerization reactions. Finally, multiplication of AgNP-labeled signal probes are localized on the electrode surface, which provide intensive electrochemical signals from highly characteristic solid-state Ag/AgCl reaction.[38]

EIS Characterization. Electrochemical impedance spectra are employed to characterize the electrode modification steps. As shown in Figure 2a, the Nyquist plot of bare gold electrode

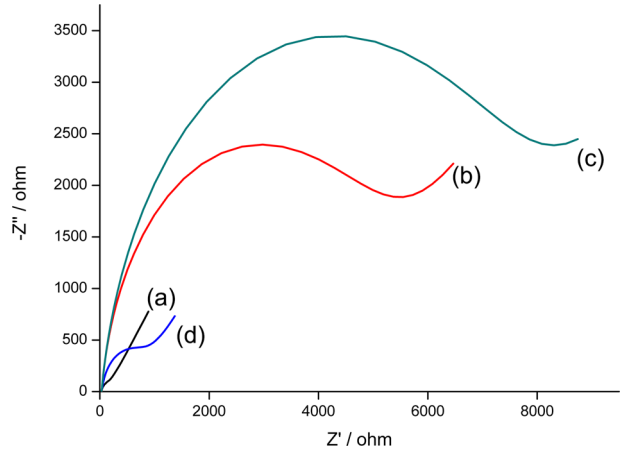

Figure 2. Nyquist diagrams of impedance spectra for (a) bare gold electrode, (b) tetrahedral DNA nanostructure modified electrode, (c) after strand displacement and catalytic recycling of microRNA with signal probe which is not labeled with AgNPs, (d) is the case using AgNP-labeled signal probe.

contains no semicircle domain, indicating limited interfacial charge transfer resistance. After the immobilization of tetrahedral DNA nanostructure, a large semicircle is observed due to electrostatic repulsion toward $Fe(CN)_6^{3-/4-}$ (Figure 2b). In the presence of microRNA and Klenow fragment, a large number of signal probes can be localized on the electrode surface. Figure 2c shows an even larger semicircle, which is ascribed to the repulsion from the hybridized signal probes without AgNPs labels. In the case of AgNP-labeled signal probe, the semicircle gets much smaller (Figure 2d). The reason is that AgNPs is oxidized to Ag^+, which facilitates the electron transfer between electrochemical species and elec-

DOI: 10.1021/acsami.5b01508
ACS Appl. Mater. Interfaces 2015, 7, 6238−6243

trode, and the interfacial charge transfer resistance declines sharply. EIS results have confirmed the electrode modification steps.

Linear Sweep Voltammetry Measurement of MicroRNA. We have then carried out LSV[39] to quantitatively determine microRNA concentration. As depicted in Figure 3,

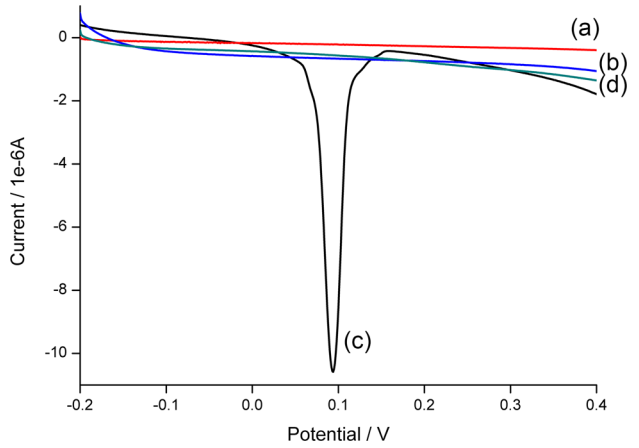

Figure 3. Linear sweep voltammograms of (a) bare gold electrode and of tetrahedral DNA nanostructure modified electrode after strand displacement reaction in the (b) absence and (c) presence of 100 fM microRNA and (d) in the presence of 100 fM microRNA using signal probe without AgNPs labels.

no current peak is present on bare gold electrode and tetrahedral DNA nanostructure modified electrode in the absence of microRNA. A sharp current peak is observed with 100 fM microRNA-mediated loop opening, signal probe immobilization and catalytic recycling (curve c). However, if the signal probe is not labeled with AgNPs, no peak appears (curve d), which demonstrates that the electrochemical signal comes from the stripping of AgNPs. Figure 4 shows the LSV curves for the detection of microRNA with a series of concentrations. The inset reveals a linear relationship between peak current and the logarithmic microRNA concentration. The fitting equation is $y = -4.646x - 71.316$ ($n = 3$, $R^2 =$ 0.995), where y is peak current and x is the logarithm of microRNA concentration. LOD is calculated to be 0.4 fM (signal-to-noise ratio of 3), which is quite low.

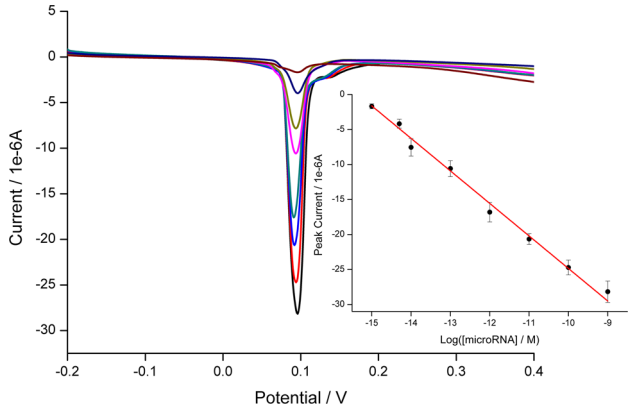

Figure 4. Linear sweep voltammograms of tetrahedral DNA nanostructure modified electrode for the detection of microRNA with the concentration of (from top to bottom) 1 fM, 5 fM, 10 fM, 100 fM, 1 pM, 10 pM, 100 pM, and 1 nM. (Inset) Calibration plot of the peak current versus the logarithmic microRNA concentration. Error bars represent standard deviations of three independent measurements.

The selectivity of this microRNA biosensor is then checked by comparing the LSV results of single-base mismatch microRNAs, which are displayed in Figure 5. The obtained

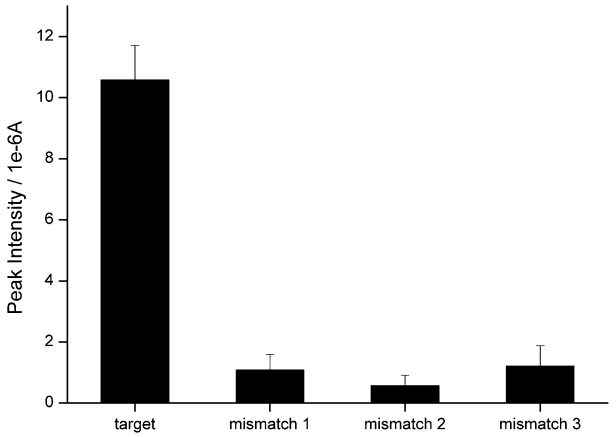

Figure 5. Comparison of LSV signal intensity in the cases of target and three single-base mismatch microRNAs with the concentration of 100 fM.

low peak currents in the cases of mismatch microRNAs demonstrate that they cannot initiate signal probe immobilization effectively, which verifies the high selectivity of this method.

Detection of MicroRNA in Human Serum Samples. Serum is a kind of samples that can be conveniently obtained and tested for the detection of different disease biomarkers. To further check the practical utility of this microRNA biosensor, serum samples from breast cancer patients are directly detected. Then, we add different amounts of target microRNA to the samples and again measure target microRNA levels by the proposed method. Table 2 shows the detected results and the recoveries, which verify that this method is accurate and can be effectively applied in biological fluids.

Table 2. Measurements of miRNA-21 in Serum Samples from Breast Cancer Patients

sample	detected (pM)	added (pM)	found (pM)	recovery (%)
serum 1	0.86	1.0	1.92	103.2
		5.0	5.99	102.2
serum 2	1.43	1.0	2.37	97.5
		5.0	6.53	101.6

CONCLUSIONS

In summary, we have fabricated an electrochemical biosensor for ultrasensitive detection of microRNA based on tetrahedral DNA nanostructure, coupled with strand displacement polymerization-mediated catalytic recycling of microRNA. The electrochemical signal originates from AgNP-based solid-state Ag/AgCl reaction on signal DNA probe. This method is simply operated and highly sensitive due to the tetrahedral DNA nanostructure and strand displacement amplification. The LOD is 0.4 fM and a wide linear range is obtained from 1 fM to 1 nM. We also examined human serum samples, and the satisfactory results demonstrate its potential practical utility

DOI: 10.1021/acsami.5b01508
ACS Appl. Mater. Interfaces 2015, 7, 6238−6243

toward microRNA assay for early diagnosis and prognosis of certain diseases.

■ ASSOCIATED CONTENT

Supporting Information

TEM image of freshly prepared AgNPs. This material is available free of charge via the Internet at http://pubs.acs.org.

■ AUTHOR INFORMATION

Corresponding Authors

*Tel.: +86 512 69588279. Fax: +86 512 69588283. E-mail: miaopeng@sibet.ac.cn.

*E-mail: tangyg@sibet.ac.cn.

Notes

The authors declare no competing financial interest.

■ ACKNOWLEDGMENTS

This work was supported by the National Natural Science Foundation of China (Grant no. 31400847) and the Natural Science Foundation of Jiangsu Province of China (Grant no. BK20141204).

■ REFERENCES

(1) Jing, Z.; Han, W. D.; Sui, X. B.; Xie, J. S.; Pan, H. M. Interaction of Autophagy with MicroRNAs and Their Potential Therapeutic Implications in Human Cancers. *Cancer Lett.* **2015**, *356*, 332−338.

(2) Yang, L.; Liu, C. H.; Ren, W.; Li, Z. P. Graphene Surface-Anchored Fluorescence Sensor for Sensitive Detection of MicroRNA Coupled with Enzyme-Free Signal Amplification of Hybridization Chain Reaction. *ACS Appl. Mater. Interfaces* **2012**, *4*, 6450−6453.

(3) Raitoharju, E.; Oksala, N.; Lehtimaki, T. MicroRNAs in the Atherosclerotic Plaque. *Clin. Chem.* **2013**, *59*, 1708−1721.

(4) Leite-Moreira, A. M.; Lourenco, A. P.; Falcao-Pires, I.; Leite-Moreira, A. F. Pivotal Role of MicroRNAs in Cardiac Physiology and Heart Failure. *Drug Discovery Today* **2013**, *18*, 1243−1249.

(5) Yin, P. T.; Shah, B. P.; Lee, K. B. Combined Magnetic Nanoparticle-based MicroRNA and Hyperthermia Therapy to Enhance Apoptosis in Brain Cancer Cells. *Small* **2014**, *10*, 4106−4112.

(6) Su, T. H.; Liu, C. H.; Liu, C. J.; Chen, C. L.; Ting, T. T.; Tseng, T. C.; Chen, P. J.; Kao, J. H.; Chen, D. S. Serum MicroRNA-122 Level Correlates with Virologic Responses to Pegylated Interferon Therapy in Chronic Hepatitis C. *Proc. Natl. Acad. Sci. U.S.A.* **2013**, *110*, 7844−7849.

(7) Kasuga, H.; Fukuyama, M.; Kitazawa, A.; Kontani, K.; Katada, T. The MicroRNA miR-235 Couples Blast-Cell Quiescence to the Nutritional State. *Nature* **2013**, *497*, 503−506.

(8) Catto, J. W. F.; Miah, S.; Owen, H. C.; Bryant, H.; Myers, K.; Dudziec, E.; Larre, S.; Milo, M.; Rehman, I.; Rosario, D. J.; Di Martino, E.; Knowles, M. A.; Meuth, M.; Harris, A. L.; Hamdy, F. C. Distinct MicroRNA Alterations Characterize High- and Low-Grade Bladder Cancer. *Cancer Res.* **2009**, *69*, 8472−8481.

(9) Jou, A. F.-J.; Lu, C.-H.; Ou, Y.-C.; Wang, S.-S.; Hsu, S.-L.; Willner, I.; Ho, J.-A. A. Diagnosing the miR-141 Prostate Cancer Biomarker Using Nucleic Acid-Functionalized CdSe/ZnS QDs and Telomerase. *Chem. Sci.* **2015**, *6*, 659−665.

(10) Tran, H. V.; Piro, B.; Reisberg, S.; Nguyen, L. H.; Nguyen, T. D.; Duc, H. T.; Pham, M. C. An Electrochemical ELISA-Like Immunosensor for MiRNAs Detection Based on Screen-Printed Gold Electrodes Modified with Reduced Graphene Oxide and Carbon Nanotubes. *Biosens. Bioelectron.* **2014**, *62*, 25−30.

(11) Wang, S. Y.; Xiang, J. B.; Li, Z. Y.; Lu, S. H.; Hu, J.; Gao, X.; Yu, L.; Wang, L.; Wang, J. P.; Wu, Y.; Chen, Z. Y.; Zhu, H. G. A Plasma MicroRNA Panel for Early Detection of Colorectal Cancer. *Int. J. Cancer* **2015**, *136*, 152−161.

(12) Mozzoni, P.; Banda, I.; Goldoni, M.; Corradi, M.; Tiseo, M.; Acampa, O.; Balestra, V.; Ampollini, L.; Casalini, A.; Carbognani, P.; Mutti, A. Plasma and EBC MicroRNAs as Early Biomarkers of Non-Small-Cell Lung Cancer. *Biomarkers* **2013**, *18*, 679−686.

(13) Dong, H. F.; Lei, J. P.; Ding, L.; Wen, Y. Q.; Ju, H. X.; Zhang, X. J. MicroRNA: Function, Detection, and Bioanalysis. *Chem. Rev.* **2013**, *113*, 6207−6233.

(14) Miao, P.; Meng, F. Y.; Wang, B. D.; Zhu, X. L.; Tang, Y. G. Highly Sensitive MicroRNA Quantification with Zero Background Signal from Silver Nanoparticles. *Electrochem. Commun.* **2015**, *51*, 89−92.

(15) Yan, L.; Yan, Y. Y.; Pei, L.; Wei, W.; Zhao, J. A G-Quadruplex DNA-Based, Label-Free and Ultrasensitive Strategy for MicroRNA Detection. *Sci. Rep.* **2014**, *4*, 7400.

(16) Chen, C. F.; Ridzon, D. A.; Broomer, A. J.; Zhou, Z. H.; Lee, D. H.; Nguyen, J. T.; Barbisin, M.; Xu, N. L.; Mahuvakar, V. R.; Andersen, M. R.; Lao, K. Q.; Livak, K. J.; Guegler, K. J. Real-Time Quantification of MicroRNAs by Stem-Loop RT-PCR. *Nucleic Acids Res.* **2005**, *33*, e179.

(17) Yang, F.; Zuo, X. L.; Li, Z. H.; Deng, W. P.; Shi, J. Y.; Zhang, G. J.; Huang, Q.; Song, S. P.; Fan, C. H. A Bubble-Mediated Intelligent Microscale Electrochemical Device for Single-Step Quantitative Bioassays. *Adv. Mater.* **2014**, *26*, 4671−4676.

(18) Miao, P.; Liu, L.; Li, Y.; Li, G. X. A Novel Electrochemical Method to Detect Mercury (II) Ions. *Electrochem. Commun.* **2009**, *11*, 1904−1907.

(19) Li, D.; Liu, J. Q.; Barrow, C. J.; Yang, W. R. Protein Electrochemistry Using Graphene-Based Nano-Assembly: An Ultra-sensitive Electrochemical Detection of Protein Molecules via Nano-particle-Electrode Collisions. *Chem. Commun.* **2014**, *50*, 8197−8200.

(20) Shin, I. S.; Chand, R.; Lee, S. W.; Rhee, H. W.; Kim, Y. S.; Hong, J. I. Homogeneous Electrochemical Assay for Protein Kinase Activity. *Anal. Chem.* **2014**, *86*, 10992−10995.

(21) Kabashima, T.; Yu, Z. Q.; Tang, C. H.; Nakagawa, Y.; Okumura, K.; Shibata, T.; Lu, J. Z.; Kai, M. A Selective Fluorescence Reaction for Peptides and Chromatographic Analysis. *Peptides* **2008**, *29*, 356−363.

(22) Tonooka, K.; Kabashima, T.; Shibata, T.; Tang, C. H.; Yu, Z. Q.; Kai, M. S. Facile Assay of Telomerase Activity Utilizing a DNA-Detectable Chemiluminogenic Reagent. *Anal. Sci.* **2008**, *24*, 471−475.

(23) Yu, Z. Q.; Kabashima, T.; Tang, C. H.; Shibata, T.; Kitazato, K.; Kobayashi, N.; Lee, M. K.; Kai, M. Selective and Facile Assay of Human Immunodeficiency Virus Protease Activity by a Novel Fluorogenic Reaction. *Anal. Biochem.* **2010**, *397*, 197−201.

(24) Miao, P.; Wang, B. D.; Yu, Z. Q.; Zhao, J.; Tang, Y. G. Ultrasensitive Electrochemical Detection of MicroRNA with Star Trigon Structure and Endonuclease Mediated Signal Amplification. *Biosens. Bioelectron.* **2015**, *63*, 365−370.

(25) Zhu, G. C.; Liang, L.; Zhang, C. Y. Quencher-Free Fluorescent Method for Homogeneously Sensitive Detection of MicroRNAs in Human Lung Tissues. *Anal. Chem.* **2014**, *86*, 11410−11416.

(26) Pawlak, M.; Grygolowicz-Pawlak, E.; Crespo, G. A.; Mistlberger, G.; Bakker, E. PVC-Based Ion-Selective Electrodes with Enhanced Biocompatibility by Surface Modification with "Click" Chemistry. *Electroanalysis* **2013**, *25*, 1840−1846.

(27) Ning, L. M.; Li, X. X.; Yang, D. W.; Miao, P.; Ye, Z. H.; Li, G. X. Measurement of Intracellular pH Changes Based on DNA-Templated Capsid Protein Nanotubes. *Anal. Chem.* **2014**, *86*, 8042−8047.

(28) Pei, H.; Wan, Y.; Li, J.; Hu, H. Y.; Su, Y.; Huang, Q.; Fan, C. H. Regenerable Electrochemical Immunological Sensing at DNA Nanostructure-Decorated Gold Surfaces. *Chem. Commun.* **2011**, *47*, 6254−6256.

(29) Lu, N.; Pei, H.; Ge, Z. L.; Simmons, C. R.; Yan, H.; Fan, C. H. Charge Transport within a Three-Dimensional DNA Nanostructure Framework. *J. Am. Chem. Soc.* **2012**, *134*, 13148−13151.

(30) Miao, P.; Tang, Y. G.; Wang, B. D.; Han, K.; Chen, X. F.; Sun, H. X. An Aptasensor for Detection of Potassium Ions Based on RecJ(f) Exonuclease Mediated Signal Amplification. *Analyst* **2014**, *139*, 5695−5699.

(31) Li, Z. H.; Zhao, B.; Wang, D. F.; Wen, Y. L.; Liu, G.; Dong, H. Q.; Song, S. P.; Fan, C. H. DNA Nanostructure-Based Universal

DOI: 10.1021/acsami.5b01508
ACS Appl. Mater. Interfaces 2015, 7, 6238−6243

Microarray Platform for High-Efficiency Multiplex Bioanalysis in Biofluids. *ACS Appl. Mater. Interfaces* **2014**, *6*, 17944−17953.
(32) Zou, B. J.; Song, Q. X.; Wang, J. P.; Liu, Y. L.; Zhou, G. H. Invasive Reaction Assisted Strand-Displacement Signal Amplification for Sensitive DNA Detection. *Chem. Commun.* **2014**, *50*, 13722−13724.
(33) Hu, Y. H.; Xu, X. Q.; Liu, Q. H.; Wang, L.; Lin, Z. Y.; Chen, G. N. Ultrasensitive Electrochemical Biosensor for Detection of DNA from *Bacillus subtilis* by Coupling Target-Induced Strand Displacement and Nicking Endonuclease Signal Amplification. *Anal. Chem.* **2014**, *86*, 8785−8790.
(34) Miao, P.; Han, K.; Sun, H. X.; Yin, J.; Zhao, J.; Wang, B. D.; Tang, Y. G. Melamine Functionalized Silver Nanoparticles as the Probe for Electrochemical Sensing of Clenbuterol. *ACS Appl. Mater. Interfaces* **2014**, *6*, 8667−8672.
(35) Miao, P.; Wang, B. D.; Han, K.; Tang, Y. G. Electrochemical Impedance Spectroscopy Study of Proteolysis Using Unmodified Gold Nanoparticles. *Electrochem. Commun.* **2014**, *47*, 21−24.
(36) Ge, Z. L.; Lin, M. H.; Wang, P.; Pei, H.; Yan, J.; Sho, J. Y.; Huang, Q.; He, D. N.; Fan, C. H.; Zuo, X. L. Hybridization Chain Reaction Amplification of MicroRNA Detection with a Tetrahedral DNA Nanostructure-Based Electrochemical Biosensor. *Anal. Chem.* **2014**, *86*, 2124−2130.
(37) Hsu, M. H.; Chuang, H.; Cheng, F. Y.; Huang, Y. P.; Han, C. C.; Chen, J. Y.; Huang, S. C.; Chen, J. K.; Wu, D. S.; Chu, H. L.; Chang, C. C. Directly Thiolated Modification onto the Surface of Detonation Nanodiamonds. *ACS Appl. Mater. Interfaces* **2014**, *6*, 7198−7203.
(38) Zhang, J.; Ting, B. P.; Jana, N. R.; Gao, Z. Q.; Ying, J. Y. Ultrasensitive Electrochemical DNA Biosensors Based on the Detection of a Highly Characteristic Solid-State Process. *Small* **2009**, *5*, 1414−1417.
(39) Meng, F. B.; Yang, J. H.; Liu, T.; Zhu, X. L.; Li, G. X. Electric Communication between the Inner Part of a Cell and an Electrode: The Way To Look inside a Cell. *Anal. Chem.* **2009**, *81*, 9168−9171.

DOI: 10.1021/acsami.5b01508
ACS Appl. Mater. Interfaces 2015, 7, 6238−6243